

# Photometric treatment of HD100453

Semester Project

Ulrich Sauter

Supervisor: Prof. Dr. Hans Martin Schmid

Co-Supervisor: Jie Ma

Department of Physics

ETH Zürich

June, 2020

## Abstract

TODO

## 1 Introduction

### 1.1 Observations

HD 100453 A, hereafter referred to HD 100453, is a Herbig Ae/Be Star with a protoplanetary disk located in the Lower Centaurus Association. HD 100453 has also an early-M star companion, called HD 100453 B. A background star is also located to the top left of Hd 100453. In this work four observations were used, all taken from the ZIMBOL imager.

One set of observation is called cyc116 and it consists of one observation with the R\_PRIM filter, central wavelength  $6.26 \cdot 10^2$  nm, and another with the I\_PRIM filter, with central wavelength of  $7.90 \cdot 10^2$  nm.

The other set, called ND4, was taken with the same filters but additionally a neutral density filter (ND4) was applied. The neutral density filter reduces the counted photons on average by a factor of  $10^{-4}$  depending on the wavelength of light.

For all observation we have 4 frames corresponding to the 4 Stokes parameters.

The radial stokes parameter

$$Q_\phi = -Q \cos 2\phi + U \sin 2\phi,$$

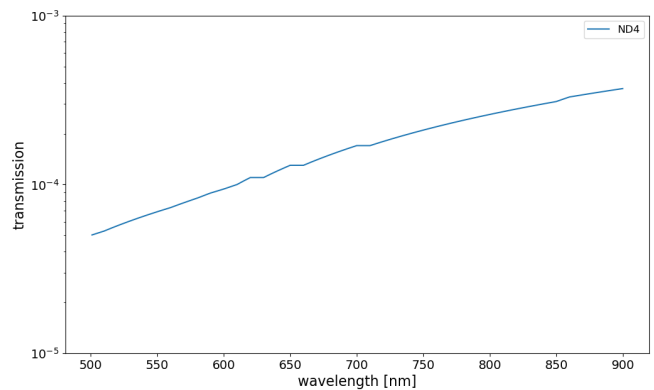
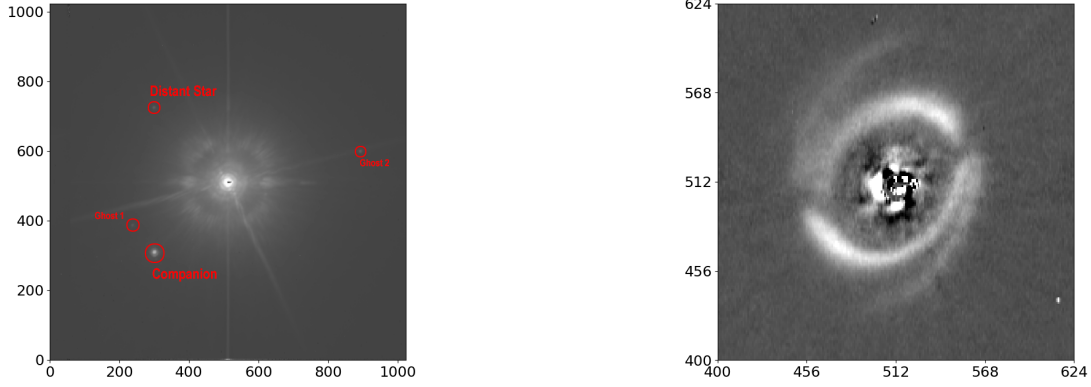


Fig. 1 Transmission coefficient of the ND4 filter.

was used, with  $\phi$  being the position angle of the location  $(x, y)$  with respect to HD 100453 at  $(x_0, y_0)$  and is written as  $\phi = \arctan \frac{x-x_0}{y-y_0}$ . For more information see [1].

Additionally we used another set of images called point spread function (PSF). The PSF describes how a point source of light is spread over the detected image.



(a)  $I_Q$  frame in the I-band of cyc116 in logarithmic scale.

(b) Zoomed in picture of the radial polarization  $Q_\phi$  of cyc116 in the I-band.

Fig. 2 (a): In the center the saturation of HD 100453 is visible by the black spot. The companion HD 100453 B is visible on the lower left of the figure. The distant star is located in the upper left. There are also two ghosts from the instrument visible.

(b): We see the disk as well as two spiral caused by the orbit of the companion.

Looking at cyc116 in figure 2a we see a problem, in the over saturation of the observation. Due to this a flux measurement is problematic. To solve this issue we have the ND4 set. There we have a faultless observation of the star but much weaker.

The first objective is to rescale the ND4 profile to match that one of cyc116 to reconstruct the peak of HD 100453. The second objective is to calculate the stellar magnitude of the objects visible in cyc116.

## 1.2 Methods

Two different methods were used to analyse the data.

### 1.2.1 Aperture Photometry

Aperture photometry is the simplest method to obtain a flux measurement of an object. It is done by integrating all the values within a circular aperture centered on the object, marked orange in figure 3, to get a total value. The size of an aperture refers the radius of the orange disk. After that, the background level needs to be subtracted. The normal way to do to this, is to calculate the average background level in an annulus around the aperture, marked red and then subtracting this average multiplied by the number of pixel in the aperture from the total value. Another way we tried to subtract the background level is by fitting a second order polynomial to the background. The final flux was then obtain by subtracting the polynomial from the aperture. We will compare these two methods in section 2.2.1 to see if the extra effort is worth.

Once all the fluxes are calculated, we can calculate the color magnitude of the objects by taking the logarithm of the flux of the I-band divided by those of the R-band. With the color

magnitude one can estimate the temperature of a star. The same procedure is also applicable to the disk of HD 100453 with a slight modification. Instead of using an circular aperture we replace it with an annular aperture to ignore the flux produced by the star.

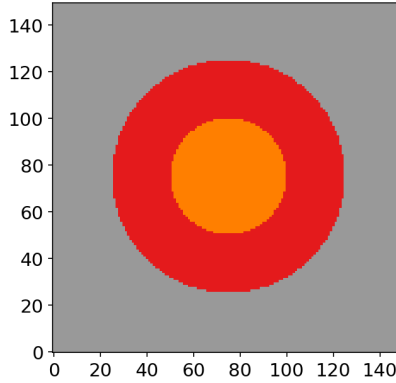


Fig. 3 Example aperture with an orange aperture and red annulus.

### 1.2.2 Azimuthal averaged profile

An azimuthal averaged profile, hereafter referred as profile, is created by averaging over all points which have the same distance from the center of the image. This makes for an appropriate data reduction method to simplify the data to 1 dimension, because we expect that the profile of the star is radial symmetric.

## 2 Data analysis

### 2.1 Isolating the disk

We worked with the profiles of the observations because it allowed us to simplify the fitting process to one dimension. First we needed to reconstruct the peak of the cyc116 profile. For that the profile of the ND4 observation needed to be rescaled to fit that of cyc116. The profile thus obtained was called the scaled profile. After this we needed to remove the emission from the star. To accomplish this, the PSF profile was fitted to the peak of the scaled profile, resulting in a profile called star profile.

#### 2.1.1 Rescaling of the ND4 profile

A simple multiplication with just a scaling factor didn't work. The reason was, that the ND4 profile is reduced by a factor of  $10^{-4}$ . So the background will also get amplified by the same factor during the rescaling. This led to unwanted results because of the high background level. To prevent this from happening, it was necessary to first subtract a constant from the profile to reduce the background level. This resulted in the following fitting function:

$$f_1(x, a, b) = a \cdot (x - b) \quad (2.1)$$

Since we were mostly interested in the reconstruction of the peak, we needed to adjust the fitting region accordingly. We excluded the first 14 data points to avoid the effect of the over saturation and also excluded the points outside a radius of 65px. We estimated the fitting parameters  $a, b$  to get good starting values for the fit. We estimated  $a$  by calculating the inverse transmission factor of the neutral density filter and  $b$  by taking the median of the background. The fitting method yielded parameters close to our estimate, which means we correctly assumed the meaning of the fitting parameters.

### 2.1.2 Fitting of the PSF

Next we fitted the PSF profile to the scaled profile. We adopted the method above with slight changes to the fitting region. Instead of the interval we used the first 32px. We only used the pixels at the peak, because the PSF profile and scaled profile had a difference away from the peak. The difference is due to the reflected light from the disk. The resulting fit matched the peak well, but the background dropped off too quickly. To counteract this behaviour we increased the fitting region by including 5 points in between 120px-200px ("tail") to control the residue of the background. To also make up for the fewer points inside the tail, the weight of those points got increased.

The fitting routine still performed poorly, due to the amplified noise of the scaled profile in the outer region. The difficulty was to choose good points for tail near the cyc116 profile. To achieve this, we tried in a first attempt to only choose points within a  $\sigma$  interval of the cyc116 profile. But still, this method resulted often in errors because for some configuration of parameters, no points were close to the cyc116 profile. We settled for a much simpler method, by creating a new mixed profile. The idea was to combine the peak of the scaled profile and use the cyc116 profile for the rest. We compared the two profiles to find a good transition point for creating the mixed profile.

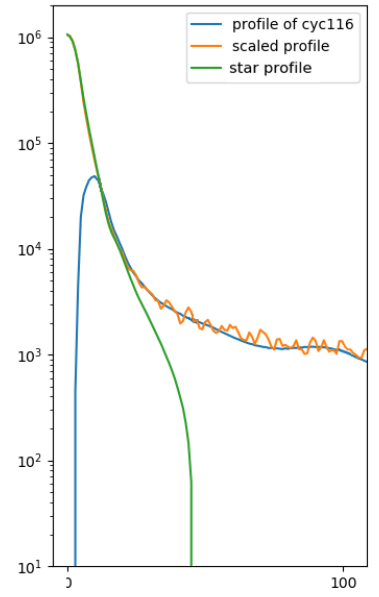


Fig. 4 Fit (green) with no additional tail.

### 2.1.3 Comparison

To compare the two profiles, we divided the cyc116 profile by the scaled profile. The result is shown in figure 5. We choose the transition to be at pixel 21. (Need to discuss). Therefore the mixed profile consisted of the first 21px of the scaled profile while the rest was the cyc116 profile. This assured us that we have a correct fit of the peak, while having good control on the background level.

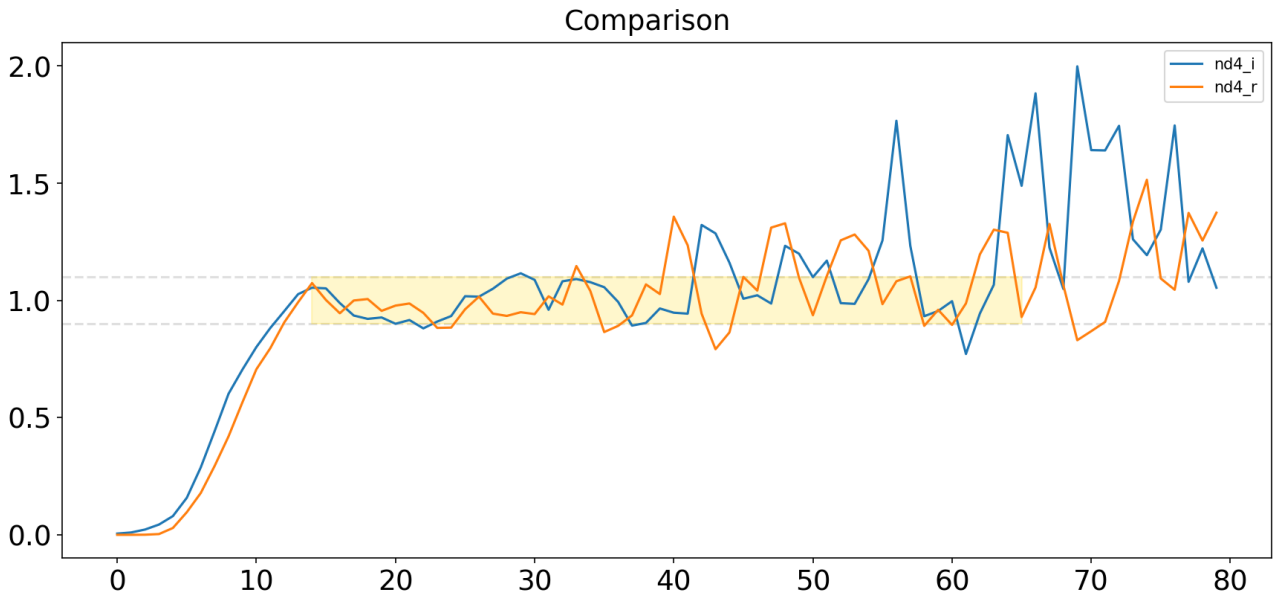


Fig. 5 The cyc116 profile divided by the scaled profile. The yellow marked region is the fitting area. The dashed lines are positioned a distance of 0.1 away from 1.

### 2.1.4 Fitting of the mixed profile

Finally to improve the fit of the PSF and adding an additional degree of freedom, we added a convolution with a Gaussian of standard deviation  $\sigma$  to the fitting method. The resulted fitting function:

$$f_2(x, a, b, \sigma) = a \cdot (gauss(x, \sigma) - b) \quad (2.2)$$

All the profiles are shown in figure 6. The results looks good but there are still some problems. One problem is that the fitted PSF profile goes sometimes over and sometimes under the profile of cyc116. This results in positive and negative values when we do the subtraction, more on that in the next section.

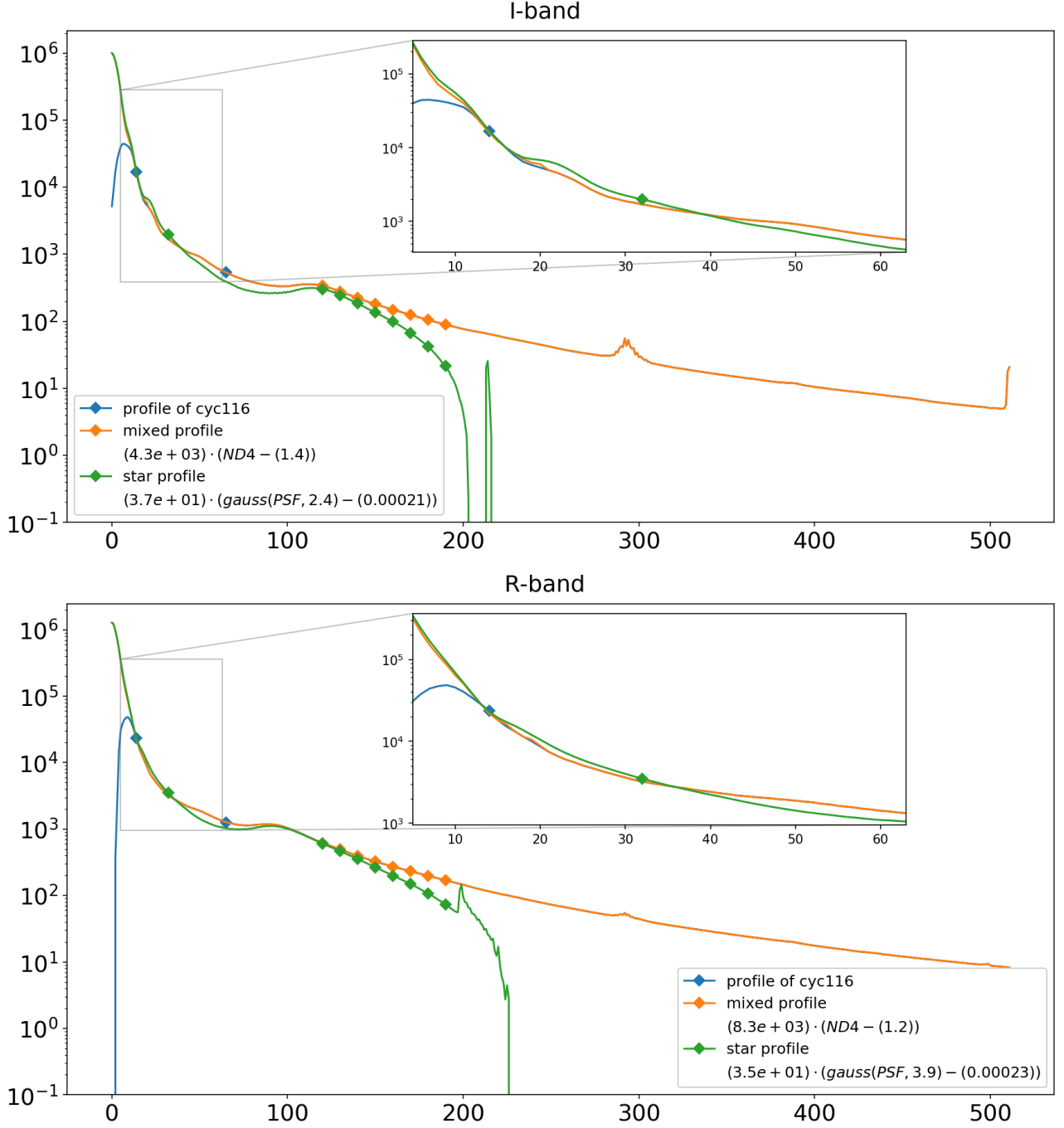


Fig. 6 The dots in the plot mark the fitting region. (Need more explanation?)

### 2.1.5 Isolating disk

For a first estimate of the disk flux we can subtract the mixed profile and star profile resulting in figure 7.

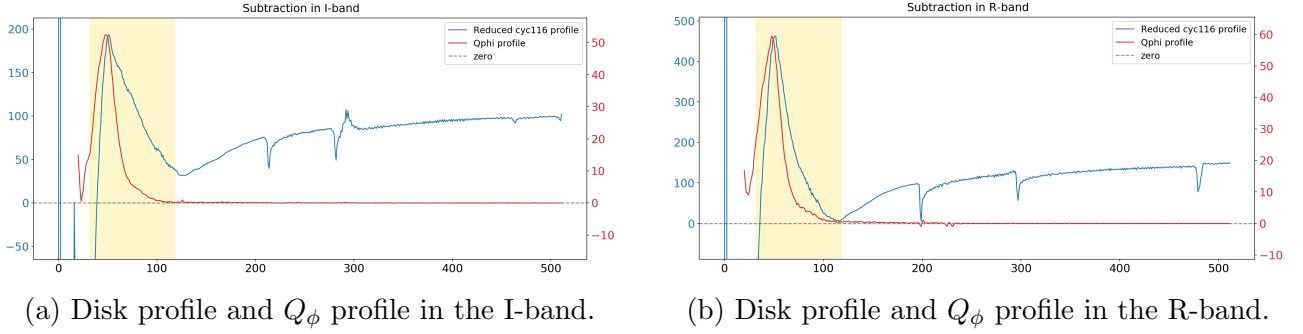


Fig. 7 The cyc116 profile subtracted by the rescaled PSF profile and the profile of  $Q_\phi$ . The points inside the yellow region were used to estimate the flux of the disk. Scale on the left for the blue line and scale on the right for the red. (Need to make Text bigger in Plot)

We can clearly see a peak around 50px, which corresponds to our disk. This is further validated by the  $Q_\phi$  profile. We also see some problems of the fit. We have a very negative signal in the first few pixels and can't clearly determine where the disk starts. We also have some kind of shift between the outside values of the cyc116 profile and the rescaled PSF profile. Which leads to the increase of the subtracted profile further out.

To get a first estimate of the flux, we summed up the values inside the yellow region and subtracted the median of the region outside of 130px.

## 2.2 Photometric Analysis

To make a complete and accurate analysis it is necessary to use a not too faint observation and one without a saturated object. To make the photometric analysis we did the following steps:

1. The flux of a big aperture needs to be calculated.  
We chose a radius of 417px which corresponds to  $3''$ .
2. Find the stellar magnitude of the central object from literature.  
In our case, it is 7.42 mag in the I-band and 7.60 mag in the R-band (table 2 of [2]).
3. Now, we can associate the flux from 1. to a stellar magnitude and determine the magnitude of the other objects. If an object has 2.5 times less flux, it has 1 less of the magnitude.
4. To get comparable results between the objects, it is important to choose the same aperture for every object.

(Maybe mention other ratios?)

### 2.2.1 Background removal

To compare the two background removal methods we will apply them on the companion and ghost 2. These objects were chosen because the surrounding of the companion is simple and the surrounding of the ghost is complex as a consequence of the spider.

For the first method in the I-band  $I_Q$ -frame, the flux is written in table 2. By changing the size of the outer annulus, the counts of the companion changes by  $\pm 2400$  and that of the ghost by

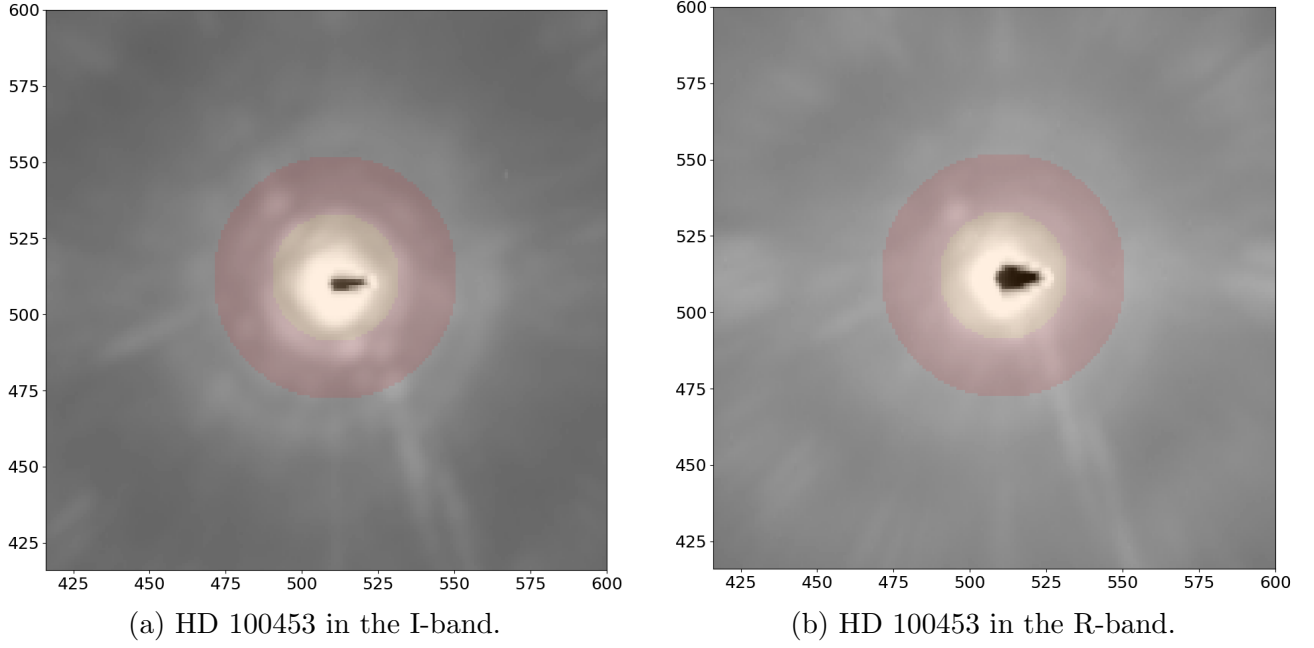


Fig. 8 HD 100453 in both bands with an aperture of size  $2.10 \cdot 10^1$  px and annulus radius of  $4.00 \cdot 10^1$  px.

$\pm 300$ .

The same size of aperture with the second method results in a flux count with background removed of  $3.89 \cdot 10^5$  for the companion and  $1.64 \cdot 10^4$ .

The values of the second method are well within a  $3\sigma$  interval of the first, meaning we don't have a significant difference between the two methods. It is better to just use the first, simpler method instead of the other.

### 2.2.2 Results?

## 3 Conclusion

TODO

## 4 References

- [1] Christian Tschudi. Dust cloud movement in r aquarii, 2018.
- [2] S. L. A. Vieira, W. J. B. Corradi, S. H. P. Alencar, L. T. S. Mendes, C. A. O. Torres, G. R. Quast, M. M. Guimares, and L. da Silva. Investigation of 131 herbig ae/be candidate stars. *The Astronomical Journal*, 126(6):2971–2987, dec 2003.

# Appendices

## A Photometrie Data

### A.1 Big aperture

Big Aperture	Counts w/o background			
	I-band		R-band	
	$I_Q$	$I_U$	$I_Q$	$I_U$
cyc116	$7.40 \cdot 10^7 \pm 0.02\%$	$7.55 \cdot 10^7 \pm 0.02\%$	$1.28 \cdot 10^8 \pm 0.02\%$	$1.31 \cdot 10^8 \pm 0.02\%$
ND4	$3.43 \cdot 10^6 \pm 39\%$	$-2.32 \cdot 10^6 \pm 70\%$	$2.32 \cdot 10^8 \pm 1\%$	$2.65 \cdot 10^8 \pm 1\%$
PSF	$4.01 \cdot 10^6 \pm 0.02\%$	$4.01 \cdot 10^6 \pm 0.02\%$	$6.78 \cdot 10^6 \pm 0.02\%$	$6.77 \cdot 10^6 \pm 0.02\%$
Mixed Profile	$1.29 \cdot 10^8 \pm 0.02\%$	$1.29 \cdot 10^8 \pm 0.02\%$	$2.04 \cdot 10^8 \pm 0.02\%$	$2.06 \cdot 10^8 \pm 0.02\%$

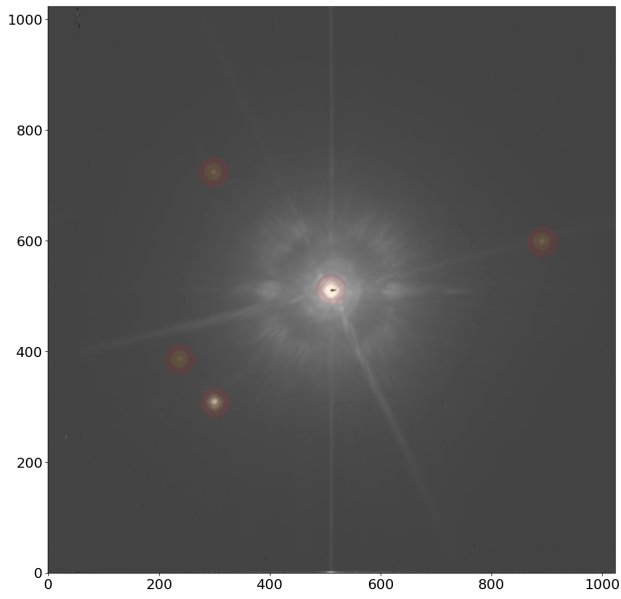
Table 1: Calculated fluxes for the big aperture of radius 416px with an outer annulus radius of 466px. The ND4 values are corrected with the associated transmission coefficient.

### A.2 Small apertures in cyc116 & disk

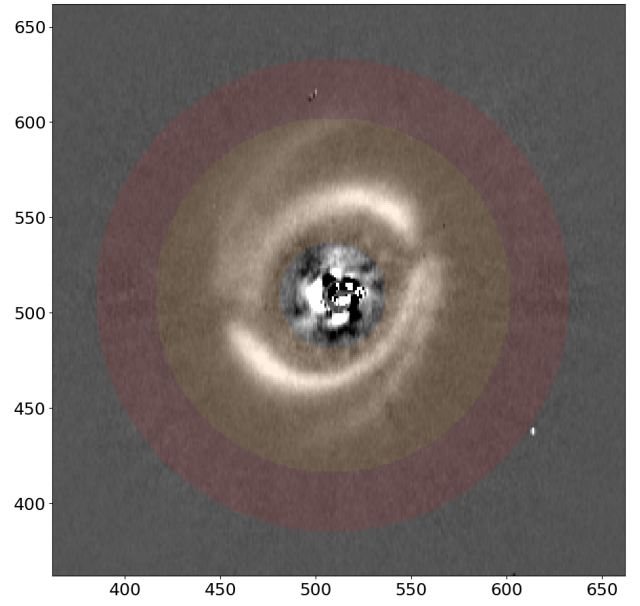
Small Aperture	Counts w/o background			
	I-band		R-band	
	$I_Q$	$I_U$	$I_Q$	$I_U$
HD 100453 A	$2.40 \cdot 10^7 \pm 2\%$	$2.40 \cdot 10^7 \pm 2\%$	$2.57 \cdot 10^7 \pm 3\%$	$2.59 \cdot 10^7 \pm 3\%$
HD 100453 B	$3.98 \cdot 10^5 \pm 0.6\%$	$3.86 \cdot 10^5 \pm 0.6\%$	$1.13 \cdot 10^5 \pm 0.5\%$	$1.09 \cdot 10^5 \pm 0.6\%$
Distant Star	$1.30 \cdot 10^4 \pm 2\%$	$1.23 \cdot 10^4 \pm 1\%$	$9.97 \cdot 10^3 \pm 1\%$	$9.54 \cdot 10^3 \pm 1\%$
Ghost 1	$6.29 \cdot 10^3 \pm 0.6\%$	$5.48 \cdot 10^3 \pm 4\%$	$5.98 \cdot 10^3 \pm 3\%$	$4.67 \cdot 10^3 \pm 4\%$
Ghost 2	$1.79 \cdot 10^4 \pm 2\%$	$1.37 \cdot 10^4 \pm 3\%$	$1.73 \cdot 10^4 \pm 4\%$	$1.19 \cdot 10^4 \pm 5\%$
Disk	$Q_\phi: 4.71 \cdot 10^5$		$Q_\phi: 4.71 \cdot 10^5$	

Table 2: Calculated fluxes for an aperture size of 20px and annulus size of 39px for the stars. The variation was calculated by moving the center of the aperture 1px in every direction as well as changing the radius by  $\pm 1$ , lastly the mean and standard deviation of the acquired values were taken. For the disk an inner radius of 28px, a middle radius of 93px and an outer radius of 124px was chosen.





(a)  $I_Q$  frame in the I-band.



(b)  $Q_\phi$  of cyc116 in the I-band.

Fig. 9 cyc116 image of  $I_Q$  and  $Q_\phi$  with marked apertures.